OPERATION MECHANISM FOR TUNABLE HEMISPHERICAL EYEBALL CAMERAS

Chaofeng Lu*, Jianliang Xiao**, Yonggang Huang***, John A. Rogers****
*Department of Civil Engineering & Soft Matter Research Center, Zhejiang University, Hangzhou, 310058, China
**Department of Mechanical Engineering, University of Colorado, Boulder, FL 80309-0427, USA
***Department of Civil and Environmental Engineering and Department of Mechanical Engineering, Northwestern University, Evanston, Illinois, 60208, USA
****Department of Materials Science and Engineering, University of Illinois,1304 West Green Street, Urbana, IL 61801, USA

Summary Systematic mechanics analyses are performed to reveal the underlying operation mechanism of a newly developed dynamically tunable hemispherical eyeball camera by using the principle of virtual work with the Yeoh material model. The predicted strain distribution, photodetector position on deformed detector surface, and the pressure-apex height relation agree well with finite element analysis and experiment. This study provides a reference for controlling and adjusting the curvature (hence the focal length and objective distance) of the eye and lens based on hyperelastic membranes during collecting high quality images.

INTRODUCTION

Imaging systems that use arrays of photodetectors in curvilinear layouts are attractive due to their ability to match the strongly nonplanar image surfaces that form with simple lenses [1,2], thereby creating new design options [3-5]. For either printing electrical components directly onto prescribed curved surfaces [3] or transferring geometrically the initially planar system onto specific curvilinear shapes [4,5], the detector curvature is fixed and the "eye" is therefore incompatible with changes in the image surface. This limitation was encompassed by a newly biomimetic design, in which photodetector arrays are integrated on transparent elastomer poly (dimethylsiloxane) (PDMS) membrane accommodating reversible deformation into hemispherical shapes with radii of curvature that can be adjusted dynamically via hydraulics [6]. Combining this type of detector with a similarly tunable fluidic planoconvex lens yields an actively tunable eyeball camera with excellent imaging characteristics, including night-vision surveillance, endoscopic imaging, and wideangle fields of view. The objective of this lecture is to study the underlying mechanism of tuning the curvature of the eye and lens (and hence the focal length and objective distance) by adjusting the pressure difference on these PDMS membranes, and therefore to provide guidance for operating this kind of eyeball camera.

MECHANICS OF TUNABLE LENS

The thickness (t=0.2 mm) of PDMS membrane for tunable lens is much smaller than the diameter (9 mm) of its deformable part confined by an open hole on the water chamber such that the membrane deforms to a convex hemispherical cap upon pumping water into the chamber. As shown in Fig. 1, the radius of the chamber is L and the apex height is H (distance between the apex and the centre of the membrane in its initial flat state), in terms of which the radius of curvature of the hemispherical cap is given by $R=(L^2+H^2)/(2H)$ and the open angle by $\varphi_m=\arcsin[2LH/(L^2+H^2)]$. Since the membrane undergoes large strain up to more than 40% in experiment, the radial and circumferential strains in the membrane due to finite deformation are $\varepsilon_r=\ln(R\varphi_m/L)$ and $\varepsilon_\theta=\ln[R\sin(r\varphi_m/L)/r]$ in the cylindrical coordinates (r,z). Finite element analysis (FEA) gives identical strain with the predicted results and thus the hemispherical shape and the analytical model is validated.

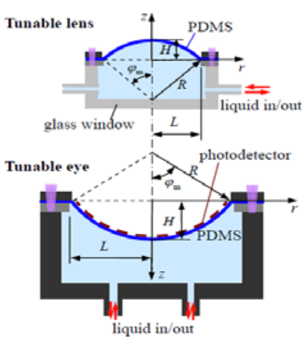

Fig. 1 Model illustration

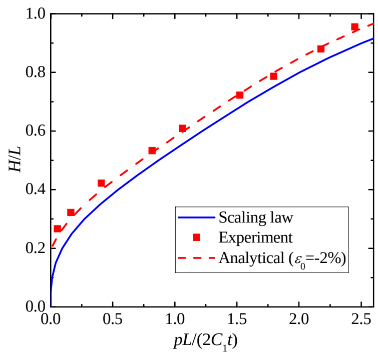

Fig. 2 Results for tunable lens

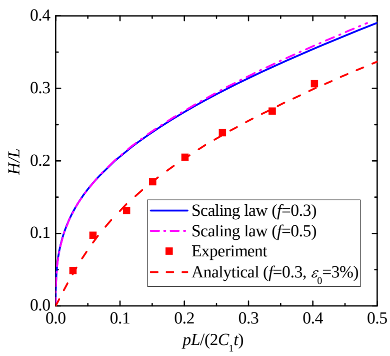

Fig. 3 Results for tunable eye

It is the pressure difference p between the two surfaces of the membrane that deform it into a hemispherical cap. We employ the principle of virtual work to determine the relationship between the pressure difference p and the apex height H of the cap, i.e. $\delta U_e-\delta W=0$, where $\delta W=p\delta V$ is the virtual work done by the pressure difference p on the virtual volume δV ($V=\pi H^2(3R-H)/3$ is the volume embraced by the hemispherical cap and the plane for the initial flat state of the membrane), and δU_e is the virtual elastic strain energy stored in the membrane on the virtual deformation δH. Due to large deformation, the elastic strain energy stored in the membrane is $U_e = 2\pi t \int_0^L \sum_{n=1}^3 C_n (I_1 - 3)^n r \mathrm{d}r$ based on the Yeoh hyperelastic material model [7], where $I_1 = \lambda_1^2 + \lambda_2^2 + \lambda_3^2$ with the principle stretch $\lambda_1 = R\varphi_m/L$, $\lambda_2 = R\sin(r\varphi_m/L)/r$, and $\lambda_3 = 1/(\lambda_1\lambda_2)$ for incompressible material, the material constants C_1=0.285 MPa, C_2=0.015 MPa, and C_3=0.019 MPa [8] for the current PDMS (sylgard 184). Upon applying the principle of virtual work, the normalized pressure difference $pL/(2C_1t)$ on the membrane is expressed as a simple function about the normalized apex height $\eta = H/L$ as

$$\frac{pL}{2C_1 t} = \frac{2}{1+\eta^2} \int_0^1 \sum_{n=1}^{3} n\bar{C}_n \left(I_1^{\text{lens}} - 3\right)^{n-1} \frac{\mathrm{d}I_1^{\text{lens}}}{\mathrm{d}\eta} \rho \mathrm{d}\rho \quad (1)$$

where $\bar{C}_n = C_n / C_1$ and $\eta = H/L$. The normalized pressure difference $pL/(2C_1t)$ versus the normalized apex height H/L is exhibited in Fig. 2, where the experiment data are also shown. The difference between the predicted results and experiment is caused by the initial strain in the membrane due to installation. According to the measurement in experiment, the analytical results with the initial strain ε_0=-2% due to squeeze compares well with experiment. Equation (1) gives the simple scaling law for tuning the lens if the membrane is made of an incompressible material with specific strengthening scheme (specific C_2/C_1 and C_3/C_1).

MECHANICS OF TUNABLE LENS AND TUNABLE EYE

The tunable eye with photodetector array (square shape of size l_{pd}=0.5 μm and spacing $l_{spacing}$=0.42 μm) integrated on a PDMS membrane (thickness t=0.4 mm) deforms to a concave hemispherical cap upon extracting water from the chamber (diameter $2L$=15 mm). The deformation profile is determined similar to the tunable lens. The hemispherical cap suggests uniform radial strain in the membrane, which implies that the photodetector initially at $(r,\theta,0)$ in cylindrical coordinates moves to $[R\sin(r\varphi_m/L), \theta, R\cos(r\varphi_m/L) - R\cos(\varphi_m)]$ after deformation. This prediction for the position of photodetector after deformation of the detector surface is validated by comparing with the FEA and experiment. Since the photodetector is several orders of magnitude more rigid than PDMS, the deformation of PDMS underneath photodetectors is neglected while that between the detectors is totally free of constrain. The principle stretch of the detector surface are $\lambda_1 = R\varphi_m / \left(L\sqrt{1-f}\right)$ and $\lambda_2 = R\sin\left(r\varphi_m/L\right) / \left(r\sqrt{1-f}\right)$, where $f = l_{pd}^2 / \left(l_{pd}^2 + l_{spacing}^2\right)$ is the area fraction of photodetectors. Upon applying the principle of virtual work based on the Yeoh hyperelastic material model, the normalized pressure difference $pL/(2C_1t)$ on the detector surface is expressed as a simple function about the normalized apex height $\eta = H/L$ as

$$\frac{pL}{2C_1 t} = \frac{2(1-f)}{1+\eta^2} \int_0^1 \sum_{n=1}^{3} n\bar{C}_n \left(I_1^{\text{eye}} - 3\right)^{n-1} \frac{\mathrm{d}I_1^{\text{eye}}}{\mathrm{d}\eta} \rho \mathrm{d}\rho \quad (2)$$

Figure 3 shows the normalized pressure difference $pL/(2C_1t)$ on the detector surface versus the normalized apex height H/L. It suggests that the area fraction of photodetectors has negligible effects on the pressure-apex height relation for small deformation. When the measured initial strain due to installation is included, the analytical results are identical to experiment.

CONCLUSIONS

In conclusion, we developed an analytical model to predict the mechanical properties of the tunable eye camera. The agreement between the predicted strain distribution, position of photodetector, and pressure-apex height relation with FEA and experiment validates the analytical model. The scaling law is very useful for controlling the pressure difference on the lens and eye surface and hence adjusting the curvature of the tunable lens and tunable eye during collecting high quality images. This analytical model is applicable to the operation of other biomimetic tunable hemispherical eyeball camera systems based on hyperelastic membranes.

References

[1] Grayson T.: Curved Focal Plane Wide Field of View Telescope Design. *Proc. SPIE* **4849**:269–274, 2002.
[2] Rim S. B. Catrysse P.B., Dinyari R., Huang K., Peumans P.: The Optical Ddvantages of Curved Focal Plane Arrays. *Opt. Express* **16**: 4965-4971, 2008.
[3] Xu X., Davanco M., Qi X.F., Forrest S.R.: Direct Transfer Patterning on Three Dimensionally Deformed Surfaces at Micrometer Resolutions and Its Application to Hemispherical Focal Plane Detector Arrays. *Org. Electron.* **9**:1122–1127, 2008.
[4] Ko H.C., Stoykovich M. P., Song J.Z., Malyarchuk V., Choi W.M., Yu C.J., Geddes J.B., Xiao J.L., Wang S.D., Huang Y.G., Rogers J.A.: A Hemispherical Electronic Eye Camera Based on Compressible Silicon Optoelectronics. *Nature* **454**:748-753, 2008.
[5] Shin G., Jung I., Malyarchuk V., Song J.Z., Wang S.D., Ko H.C., Huang Y.G., Ha J.S., Rogers J.A.: Micromechanics and Advanced Designs for Curved Photodetector Arrays in Hemispherical Electronic-Eye Cameras. *Small* **6**:851-856, 2010.
[6] Jung I., Xiao J.L., Malyarchuk V., Lu C.F., Li M., Liu Z.J., Yoon J.S., Huang Y.G., Rogers J.A.: Dynamically Tunable Hemispherical Electronic Eye Camera System with Adjustable Zoom Capability. *Proc. Nat. Acad. Sci. USA* **108**:1788-1793, 2011.
[7] Schneider F., Fellner T., Wilde J., Wallrabe U.: Mechanical Properties of Silicones for MEMS. *J Micromech Microeng* **18**:065008, 2008.
[8] Yeoh O.H.: Some Forms of The Strain Energy Function for Rubber. *Rubber Chem Technol* **66**:754-771, 1993.